Macromolecules **2007,** *40,* 6464−6472

Successful Chain Extension of Polyacrylate and Polystyrene Macroinitiators with Methacrylates in an ARGET and ICAR ATRP

Laura Mueller, Wojciech Jakubowski, Wei Tang, and Krzysztof Matyjaszewski*

Center for Macromolecular Engineering, Department of Chemistry, Carnegie Mellon University, 4400 Fifth Avenue, Pittsburgh, Pennsylvania 15213

Received May 18, 2007; Revised Manuscript Received June 8, 2007

ABSTRACT: Well-defined block copolymers poly(*n*-butyl acrylate)-*b*-poly(methyl methacrylate-*co*-styrene) and polystyrene-*b*-poly(methyl methacrylate-*co*-styrene) were synthesized using activators regenerated by electron transfer (ARGET) and initiators for continuous activator regeneration (ICAR) for atom transfer radical polymerization (ATRP). In order to overcome the poor initiation efficiency of polystyrene and poly(*n*-butyl acrylate) macroinitiators during chain extension with methacrylates, a small amount of styrene was used as a comonomer in the second block. To determine the percentage of styrene necessary for efficient chain extension, studies with low molecular weight alkyl halide initiators that model the poly(*n*-butyl acrylate) and polystyrene macroinitiators, respectively, were performed. Extension from the macroinitiators was then conducted using the appropriate methyl methacrylate/styrene comonomer mixture to obtain well-defined block copolymers, for example, starting from poly(*n*-butyl acrylate) macroinitiator ($M_n = 18\,000$, $M_w/M_n = 1.12$), a poly(*n*-butyl acrylate)-*b*-poly(methyl methacrylate-*co*-styrene) ($M_n = 39\,100$, $M_w/M_n = 1.23$) was obtained. Without styrene, a block copolymer with a bimodal molecular weight distribution was formed: poly(*n*-butyl acrylate)-*b*-poly(methyl methacrylate): $M_n = 36\,400$, $M_w/M_n = 1.70$). Computational simulations also indicated that the improved initiation efficiency was due to higher concentration of Cu^I species caused by lower K_{ATRP} of polystyrene chain ends.

Introduction

Block copolymers are an interesting class of materials that possess different and often desirable properties compared to those of each individual homopolymer segments they are comprised of.[1,2] Block copolymers are used commercially, for example, as thermoplastic elastomers, adhesives, or surfactants. Well-defined block copolymers are synthesized through various living polymerization methods.[3] Living ionic and coordination polymerizations are highly moisture sensitive, and strict conditions are required to conduct such reactions. Controlled radical polymerizations, on the other hand, have proved to be versatile in the synthesis of a variety of block copolymers and other more complex architectures. These methods include nitroxide-mediated polymerization (NMP),[4] reversible addition fragmentation chain transfer polymerization (RAFT),[5] and atom transfer radical polymerization (ATRP).[6−9] ATRP is an especially robust system that can be used to form a wide range of polymers and copolymers under a wide range of reaction conditions.[10−13]

To form a block copolymer by ATRP, a macroinitiator chain capped with a halogen (P_n-X) is activated by Cu^I-X/ligand, and extended with monomer (M) (Scheme 1). A very important condition to obtain a well-defined block copolymer is that the apparent rate constant of initiation should be greater than that of propagation, if the system is fully equilibrated.[13−15] In other words, $K_{ATRP}^{initiator}k_i > K_{ATRP}^{monomer}k_p$, where k_i and k_p are the rate constants for reinitiation (crosspropagation) and propagation, respectively, and $K_{ATRP} = k_{act}/k_{deact}$. This ensures that all P_n-X chains begin growth within a narrow time frame, and a product with a narrow distribution of molecular weights is obtained. There are, however, certain cases where this condition is not met. For example, observed values of K_{ATRP} for tertiary alkyl halides are generally much larger than those for secondary alkyl halides,[16] and such a system may not reach equilibrium. Consequently, there is poor initiation efficiency in the ATRP of methacrylate monomer from acrylate or styrene-based (macro)initiators ($K_{ATRP}^{initiator}k_i < K_{ATRP}^{monomer}k_p$). At the beginning of such a block copolymerization, a small fraction of polyacrylate or polystyrene macroinitiator terminal halogens are activated, methacrylate monomer is added, then the chain is deactivated again to be capped with a halogen. The resulting dormant chain is much more likely to reactivate compared to the remaining unactivated polyacrylate or polystyrene macroinitiator. This leads to an inefficient extension of the macroinitiator, and a product with a bimodal distribution of molecular weights is obtained.

A procedure was developed to overcome poor initiation efficiency in a standard ATRP. The method, known as “halogen exchange”, utilizes a bromide terminated initiator used in conjunction with a CuCl-based catalyst complex.[15,17,18] Initiation of the R−Br bond occurs, followed by propagation with methacrylate, and then deactivation with Cu^{II} catalyst to form $R-P_n-Cl$ dormant chains. K_{ATRP} values for an R−Cl species are smaller than those for an R−Br species.[16] So for this system, $K_{ATRP}^{initiator}k_i > K_{ATRP}^{monomer}k_p$. Initiators contain a more reactive R−Br bond while dormant, reacted chains mostly contain the less-labile R−Cl bond. Therefore, a more equivalent amount of initiation will occur relative to propagation, resulting in improved initiation efficiency. Halogen exchange has been successfully applied to a number of systems where the addition of the second monomer would form a more active chain end than that present on the added (macro)initiator.[15,17−25]

Recently, methods to conduct ATRP with very low catalyst concentrations have been developed. These methods, known as activators regenerated by electron transfer (ARGET) and initiators for continuous activator regeneration (ICAR) have allowed polymerization to occur with as low as only a few parts per million of copper.[26−32] In ATRP, termination reactions may occur not only via biradical coupling/disproportionation that lead to the accumulation of Cu^{II} deactivator species, but also via

---

* Corresponding author. E-mail: km3b@andrew.cmu.edu.

10.1021/ma071130w CCC: $37.00

Scheme 1. Mechanism for Atom Transfer Radical Polymerization (ATRP)

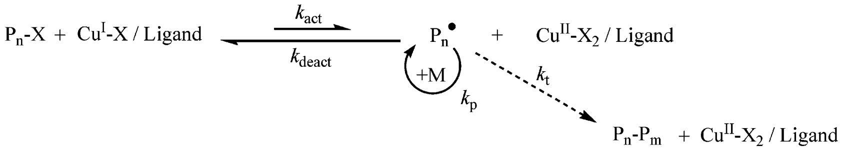

Scheme 2. Mechanism for Activators Regenerated by Electron Transfer for Atom Transfer Radical Polymerization (ARGET ATRP)

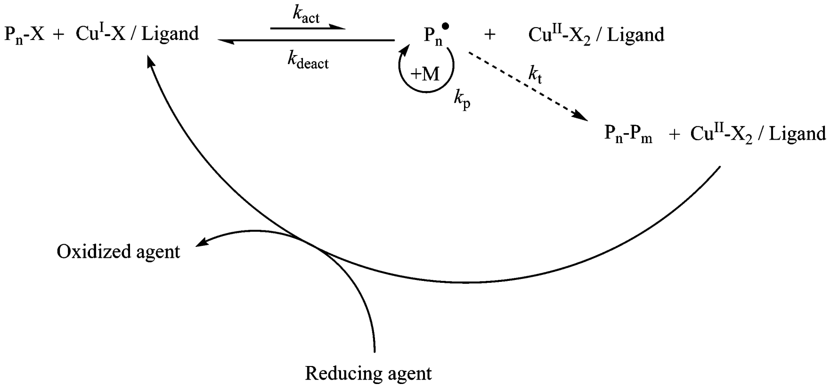

outer sphere electron transfer between growing radicals and copper species.[33−35] To overcome the latter problem, ARGET ATRP employs a very small amount of copper that is continuously regenerated to the Cu^I activator state by an excess of an appropriate reducing agent (Scheme 2). ICAR similarly regenerates Cu^I, but through the use of an organic radical initiator, such as AIBN. It has been shown that ARGET and ICAR are successful polymerization methods to obtain well-defined polymers and block copolymers.[29] ARGET has also been shown to improve the synthesis of high molecular weight polymers via ATRP.[26,30] The benefit of low copper concentration makes ARGET and ICAR very attractive processes for many applications, however it leads to some challenges. Because there is such a low amount of copper catalyst compared to the concentration of initiating sites, halogen exchange cannot be effective. Therefore, a new technique should be developed in order to ensure efficient cross-propagation in the extension of methacrylates from polyacrylate and polystyrene macroinitiators.

Charleux et al. recently reported a process for the synthesis of methacrylate-rich polymers and block copolymers via NMP.[36,37] The NMP of methacrylates is difficult due to the formation of an unstable bond between the terminal methacrylate unit and the mediating nitroxide radical. But, adding a small percentage of styrene provided enough control over the system to keep it “living”, due to its formation of a much more stable bond with nitroxides. It was thought that the use of styrene or *n*-butyl acrylate as a comonomer could also be applied to certain ARGET and ICAR systems with poor initiation efficiency. The concept was that by adding a fraction of styrene or *n*-butyl acrylate to the chain extension of a polyacrylate or polystyrene macroinitiator with a substituted methacrylate, a vast improvement in control could be achieved. A styrene or *n*-butyl acrylate end group is less reactive than a methacrylate end group, therefore incorporation of such a comonomer would lead to dormant chains with an activity near equivalent to that of the macroinitiator. Growth of the polymer chains would be comparable to unextended macroinitiator, eliminating the problem of poor initiation efficiency. However, another important parameter is the relative rate of incorporation of the comonomer. Apparently, *n*-butyl acrylate incorporates too slowly to act as a successful mediator. Styrene, on the other hand, is much more efficient.

In this paper, the synthesis of block copolymers by ARGET and ICAR ATRP where the first block is poly(*n*-butyl acrylate) or polystyrene and the second block is formed from a methyl methacrylate/styrene comonomer mixture is reported. Model reactions from small molecule initiators were performed to determine the optimal amount of styrene needed for the reaction, and computer simulations were performed to support these results and better understand the active process.

Experimental Section

Chemicals. Methyl methacrylate (MMA) (Acros, 99%), styrene (St) (Aldrich, 99%), and *n*-butyl acrylate (BA) (Acros 99+%) were passed through a column filled with basic alumina to remove inhibitor. Tris(2-pyridylmethyl)amine (TPMA) was synthesized following the previously reported procedure.[38] Anisole (Aldrich, 99%), azobis(isobutyronitrile) (AIBN) (Aldrich, 98%), copper(II) bromide (Acros, 99%), copper(II) chloride (Acros, 99%), ethyl 2-bromoisobutyrate (EBriB) (Acros, 98%), methyl 2-bromopropionate (MBrP) (Aldrich, 98%), 1-phenylethyl bromide (PEBr) (Aldrich, 97%), and tin(II) 2-ethylhexanoate ($Sn(EH)_2$) (Aldrich, 95%), were used as received.

Synthesis of Poly(MMA-*co*-St) and PolyMMA Using ARGET ATRP from MBrP and PEBr as Model Studies. General procedure for ARGET ATRP (50 ppm of Cu catalyst, targeted number-average degree of polymerization (DP_n) = 200): MMA (2.0 mL, 18.7 mmol) and St (0.24 mL, 2.08 mmol) were purged with nitrogen gas and transferred via purged syringes to a dry, 10 mL nitrogen-purged Schlenk flask. A solution of $CuCl_2$ (0.14 mg, 1.04 μmol) and TPMA (1.8 mg, 6.24 μmol) in purged anisole (1 mL) was added. The resulting mixture was stirred for 10 min, and then a purged solution of MBrP (12 μL, 0.104 mmol) in anisole (1 mL) was added. $Sn(EH)_2$ (3.4 μL, 0.0104 mmol) in purged anisole (0.5 mL) was then added to begin polymerization. An initial sample was taken via purged syringe, and the sealed flask was placed in an oil bath at 90 °C. Samples were taken at timed intervals and analyzed by gas chromatography (GC) and gel-permeation chromatography (GPC) to follow the progress of the reaction. The polymerization was stopped by opening the flask and exposing the catalyst to air. This procedure was repeated for 0% St and 20% St; 0% St, 10% St, and 20% St reactions were performed using PEBr as initiator.

Synthesis of PolyBA and PolySt Macroinitiators. Purged BA (15 mL, 105 mmol) was transferred via a purged syringe to a dry, 10 mL nitrogen-purged Schlenk flask. A solution of $CuBr_2$ (1.1 mg, 0.00512 mmol) and TPMA (5.7 mg, 0.0197 mmol) in degassed anisole (1 mL) was added. The resulting mixture was stirred for 10 min, and then a purged solution of EBriB (96 μL, 0.657 mmol) in anisole (1 mL) was added. $Sn(EH)_2$ (21 μL, 0.0657 mmol) in purged anisole (1 mL) was added to begin polymerization. An initial sample was taken via purged syringe, and the sealed flask was placed in an oil bath at 60 °C. Samples were taken at timed intervals and analyzed by GC and GPC to follow the progress of the reaction. The polymerization was stopped by opening the flask and exposing the catalyst to air. The mixture was diluted with 20 mL of THF and passed through a neutral alumina column. Solvent and monomer were evaporated to yield pure polyBA macroinitiator. A similar procedure was used to synthesize polySt macroinitiator.

Synthesis of PolyBA-*b*-Poly(MMA-*co*-St) and PolySt-*b*-Poly-(MMA-*co*-St). PolyBA−Br (1 g, 0.0556 mmol) and anisole (1 mL) were added to a Schlenk flask, and purged with nitrogen. Next, MMA (1.1 mL, 10.0 mmol) and St (0.13 mL, 1.11 mmol) purged with nitrogen were added to the flask, followed by $CuCl_2$ (0.075 mg, 0.556 μmol) and TPMA (0.97 mg, 3.33 μmol) in purged anisole (0.5 mL). $Sn(EH)_2$ (1.8 μL, 5.56 μmol) in purged anisole (0.5 mL) was added to begin polymerization. An initial sample was taken via purged syringe, and the sealed flask was placed in an oil bath at 90 °C. Samples were taken at timed intervals and analyzed by GC and GPC to follow the progress of the reaction. The polymerization was stopped by opening the flask and exposing the catalyst to air, and polyBA-*b*-poly(MMA-*co*-St) was obtained. A similar procedure was used to synthesize polySt-*b*-poly(MMA-*co*-St). For synthesis of PolyBA-*b*-Poly(MMA-*co*-St) by initiators for continuous activator regeneration (ICAR) ATRP, 5.56 μmol of AIBN was added in place of $Sn(EH)_2$, 0.556 μmol of TPMA was used, and the oil bath was thermostated at 60 °C.

Characterization. Monomer conversions were determined from the concentration of the unreacted monomer in the samples periodically removed from the reactions using a Shimadzu GC-14A gas chromatograph, equipped with a capillary column (DB-Wax, 30 m × 0.54 mm × 0.5 μm, J&W Scientific). Anisole was used as an internal standard for calculation of monomer conversions. The polymer samples were measured by GPC (Polymer Standards Services (PSS) columns (guard, 10^5, 10^3, and 10^2 Å), with THF eluent at 35 °C, flow rate = 1.00 mL/min, and differential refractive index (RI) detector (Waters, 2410)). Toluene was used as the internal standard to correct the fluctuation of the THF flow rate. The apparent molecular weights and polydispersity were determined with a calibration based on linear polystyrene and poly(methyl methacrylate) standards using WinGPC 6.0 software from PSS.

Simulations. The PREDICI program (version 6.3.1) was used for all kinetic modeling; it employs an adaptive Rothe method as a numerical strategy for time discretization. The concentrations of all species can be followed with time.

Results and Discussion

In a typical ARGET or ICAR ATRP, the concentration of copper catalyst is close to 50 ppm. This amount of copper is about 100 times lower than that of the added initiator. Accordingly, only 1% of chains could be involved in halogen exchange and this procedure cannot be successful for these systems. It was anticipated the addition of a less active comonomer would provide the needed control in the initial stages of polymerization. Several reactions were performed using both *n*-butyl acrylate and styrene as the comonomer for ARGET ATRP. It was found that styrene gave better results and was subsequently used as a comonomer for the successful extension of poly(*n*-butyl acrylate) and polystyrene macroinitiators with methyl methacrylate. A poly(*n*-butyl acrylate) macroinitiator was also extended using ICAR ATRP with methyl methacrylate and the same ratio of styrene comonomer. Predici simulations were also performed to better understand the experimental findings.

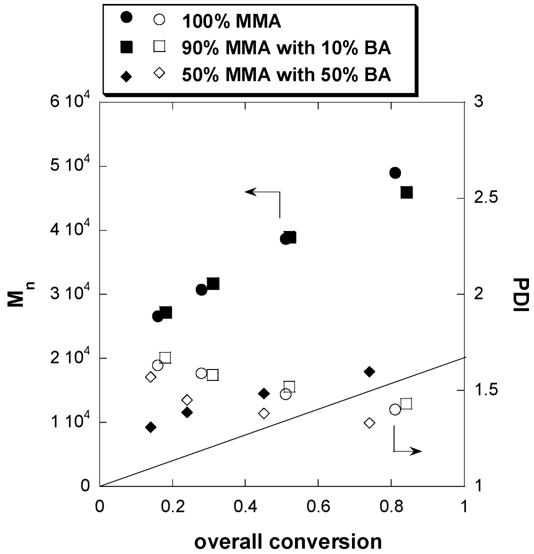

Figure 1. Molecular weight (M_n) and polydispersity (PDI) as a function of conversion in ARGET ATRP of methyl methacrylate with 0 (●, ○), 10 (■, □), and 50 (◆, ◇) mol % butyl acrylate using 50 ppm of copper in the presence of MBrP initiator. Experimental conditions for polymerization of MMA with 10 mol % of BA: $MMA/BA/MBrP/CuCl_2/TPMA/Sn(EH)_2 = 180/20/1/0.01/0.06/0.1$; $[MMA]_0 = 4.2$ M; $T = 90$ °C, in anisole (0.5 volume equivalents vs monomer).

Synthesis of Poly(MMA-*co*-BA) using ARGET ATRP from MBrP as a Model Study. The concept of using a less active comonomer to improve efficiency of cross-propagation in ARGET ATRP systems was first tested with *n*-butyl acrylate (BA). Starting from methyl 2-bromopropionate (MBrP) (a secondary alkyl halide with a structure resembling a polyacrylate chain end), various ratios of methyl methacrylate (MMA) and BA were polymerized under ARGET conditions. In the polymerization with 100% MMA, it was found that initiation efficiency was very poor, as expected (Figure 1). The molecular weight as determined by GPC was several times higher than the predicted value (determined by multiplying conversion with the target molecular weight). This means not all of the chains were initiated at the beginning of the reaction and that polymerization progresses by preferentially reactivating molecules with terminal methacrylate monomer units. In the polymerization of MMA with 10 mol % BA, no significant improvement in control was seen, as the molecular weight was still much higher than predicted (Figure 1). At 50% monomer conversion, initiation efficiency (calculated from the ratio of theoretical molecular weight to molecular weight as determined by GPC) was less than 25%. Using a much higher concentration of BA (50 mol % BA vs MMA), molecular weights shifted closer to the theoretical values and initiation efficiency approached 75%, however the results were still not desirable as such a large ratio of BA was needed. Thus, BA was found not to be the appropriate choice for efficient cross propagation.

At steady state in the free radical copolymerization of acrylates with methacrylates, $[M][A^*]k_{AM} = [A][M^*]k_{MA}$ (where [M] and [M*] are methacrylate and methacrylate radical concentrations, respectively, and [A] and [A*] are acrylate and acrylate radical concentrations, respectively). The rate constants of cross-propagation, calculated from the known reactivity ratios and homopropagation rate constants, differ greatly between these two monomers ($k_{AM} \sim 200\ k_{MA}$).[39−41] Therefore, even at the equimolar concentration of both comonomers, only 0.5% of growing chains have acrylate radical structure and 99.5% of chains have methacrylate structure. At 10 mol % of BA, the former value decreases to 0.05%. Consequently, the chance that

Table 1. Experimental Conditions and Properties of PMMA and P(MMA-*co*-St) Prepared by ARGET ATRP, Using MBrP and PEBr as Initiator[a]

entry	initiator	monomer ratio MMA/St	mol % St	time (min)	convn (%) MMA/St	$M_{n,theo}$[b] (g/mol)	$M_{n,GPC}$ (g/mol)	M_w/M_n
1	MBrP	200/−	0	1080	72/−	14 400	62 000	1.34
2	MBrP	180/20	10	900	79/94	16 100	26 300	1.38
3	MBrP	160/40	20	960	59/78	12 500	28 300	1.36
4	PEBr	200/−	0	1000	78/−	16 000	47 800	1.31
5	PEBr	180/20	10	980	91/99	18 500	27 800	1.48
6	PEBr	160/40	20	1025	83/95	17 300	28 000	1.43

[a] Experimental conditions: monomer/initiator/$CuCl_2$/TPMA/$Sn(EH)_2$ = 200/1/0.01/0.06/0.1; $[monomer]_0 = 4.67$ M; $T = 90$ °C, in anisole (0.5 volume equivalent vs monomer). [b] $M_{n,\ theo} = ([monomer]_0/[initiator]_0) \times$ conversion $\times M_{monomer}$.

A* will be deactivated to form dormant species is very small compared to M* being deactivated, even if the deactivation rate constant could be ~10 times higher for acrylate-derived radical.[42] Therefore, the presence of acrylate cannot help to slow propagation of the second block and control over the reaction is poor. Styrene (St), on the other hand, could be a better candidate. The rate constants of cross-propagation are nearly equal between methacrylates and St ($k_{MSt} \sim k_{StM}$).[40,41] Because of this, St is much more likely to be on a dormant chain end than BA in comparison with MMA, and the reaction will proceed as desired. An added benefit to the use of St, is that the glass transition temperature (T_g) is closer to that of MMA than compared to BA (MMA, $T_g = 120$ °C; BA, $T_g = -54$ °C; St, $T_g = 100$ °C).[43] St should therefore be a better candidate, especially for the synthesis of thermoplastic elastomers.

Synthesis of Poly(MMA-*co*-St) Using ARGET ATRP from MBrP and PEBr as Model Studies. Several ARGET copolymerizations were performed with various ratios of St to MMA using both MBrP and 1-phenylethyl bromide (PEBr) in order to model the appropriate amount of St required for efficient extension of poly(*n*-butyl acrylate) (PBA) and polystyrene (PSt) macroinitiators with MMA. Polymerizations with 0, 10, and 20 mol % St were performed for each MBrP and PEBr, and these are summarized in Table 1. It was anticipated that the presence of a greater concentration of St during the preparation of the copolymer, the better the control over the initiation step. Initiation from both MBrP and PEBr is slower than propagation of MMA. If St monomer is present, it should be statistically added to a growing chain and will be present at the terminus of a growing copolymer chain. Once there, it again forms a similar secondary alkyl-halide bond to that present in the remaining initiator. Propagation then becomes comparable to the rate of initiation, and hence initiation is improved. Indeed, this result is observed.

When no St is present in the reaction medium, the molecular weight, as determined by GPC, is 3−4 times higher than predicted, indicating poor initiation efficiency. When as little as 10 mol % St was added as a comonomer, the actual molecular weight was only about 1.5 times higher than theory. This indicates that the presence of St greatly improves control over the polymerization from each MBrP and PEBr. Figure 2 depicts the growth of molecular weight with respect to conversion for both the ARGET of pure MMA and of 90 mol % MMA with 10 mol % St. The presence of St gives molecular weights much closer to the theoretical values. Initiation efficiency does not change with conversion and is about 80%. The polydispersities of the copolymers obtained in each reaction are comparable.

The reactivity ratios between St and MMA are both smaller than unity, showing a tendency for alternation. Therefore, when there is a smaller fraction of styrene in the copolymerization, it is used up faster, as seen in Figure 3. This is a potential problem as the presence of styrene provides control throughout the polymerization. In the case of 10 mol % St, MMA reached high conversion before all the styrene disappeared. However, the polydispersity increased toward the end, indicating a slight loss of control. Since this problem does not occur until the end of the polymerization, it will not affect initiation efficiency. If control is desired toward higher conversions, a gradual, continuous feed of styrene monomer throughout the reaction could improve the system. These results indicate that for styrene, more chain ends can be converted to less active halogen-capped dormant species than for acrylate, used as comonomer.

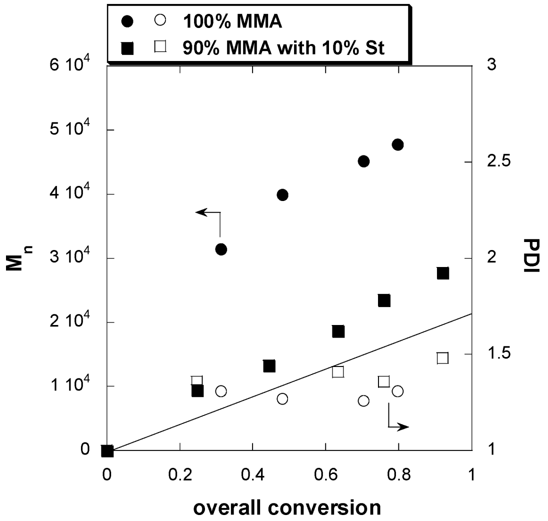

Figure 2. Molecular weight (M_n) and polydispersity (PDI) as a function of conversion in ARGET ATRP of methyl methacrylate 0 (●, ○), and 10 mol % styrene (■, □) using 50 ppm of copper in the presence of PEBr initiator. Experimental conditions for polymerization of MMA with 10 mol % of St: MMA/St/PEBr/$CuCl_2$/TPMA/$Sn(EH)_2$ = 180/20/1/0.01/0.06/0.1; $[MMA]_0 = 4.2$ M; $T = 90$ °C, in anisole (0.5 volume equivalents vs monomer).

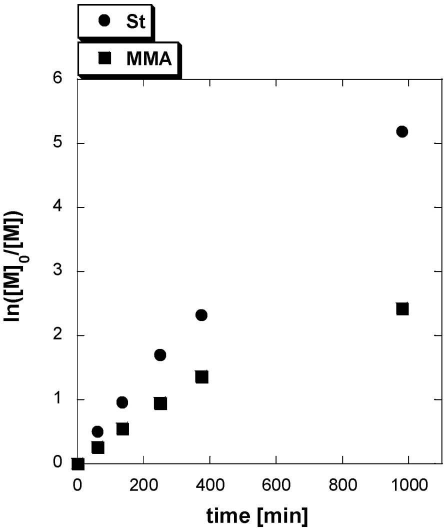

Figure 3. Semilogarithmic kinetic plot of the ARGET ATRP of methyl methacrylate with 10 mol % styrene using 50 ppm of copper in the presence of PEBr initiator. Experimental conditions: MMA/St/PEBr/$CuCl_2$/TPMA/$Sn(EH)_2$ = 180/20/1/0.01/0.06/0.1; $[MMA]_0 = 4.2$ M; $T = 90$ °C, in anisole (0.5 volume equivalents vs monomer).

Synthesis of Poly(*n*-butyl acrylate)-*b*-poly(methyl methacrylate-*co*-styrene) and Polystyrene-*b*-poly(methyl methacrylate-*co*-styrene). The PSt and PBA macroinitiators were synthesized under typical ARGET conditions (PSt, $M_n = 19\,500$,

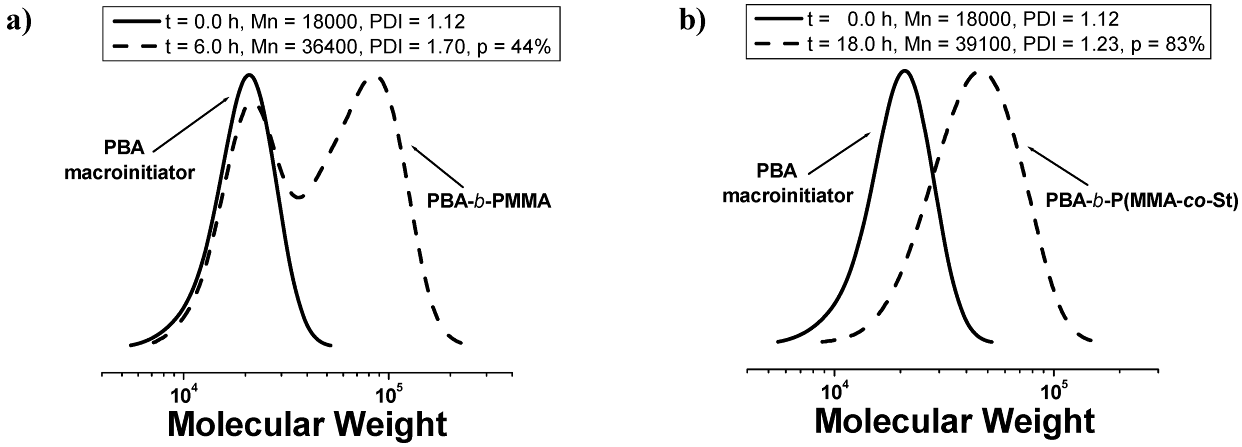

Figure 4. GPC traces of PBA−Br macroinitiator before and after chain extension with (a) MMA and (b) MMA/St copolymer. Experimental conditions for chain extension with MMA and 10 mol % St: MMA/St/PBA−Br/CuCl$_2$/TPMA/Sn(EH)$_2$ = 180/20/1/0.01/0.06/0.1; [MMA]$_0$ = 2.5 M; T = 90 °C, in anisole (0.75 volume equivalents vs monomer).

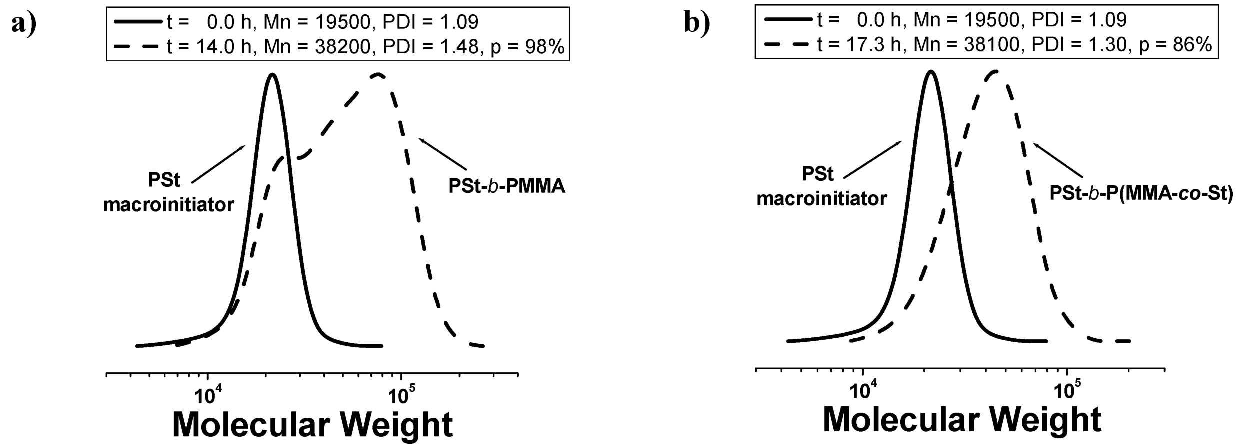

Figure 5. GPC traces of PSt-Br macroinitiator before and after chain extension with (a) MMA and (b) MMA/St copolymer. Experimental conditions for chain extension with MMA and 10 mol % St: MMA/St/PSt-Br/CuCl$_2$/TPMA/Sn(EH)$_2$ = 180/20/1/0.01/0.06/0.1; [MMA]$_0$ = 2.5 M; T = 90 °C, in anisole (0.75 volume equivalents vs monomer).

M_w/M_n = 1.09; PBA, M_n = 18 000, M_w/M_n = 1.12).[27] Each of the macroinitiators was extended with both pure MMA and with the mixture of 90 mol % MMA/10 mol % St. It is clearly seen in Figures 4 and 5 that with no St present, there is a bimodal distribution of molecular weights. This is a clear indication of poor initiation efficiency of the macroinitiators. With St present, a clean shift of the GPC trace occurs. The polydispersity of each the PSt and PBA extensions increase slightly through the reaction, which could be again attributed to the faster consumption of styrene throughout polymerization. The extension of PBA macroinitiator is more difficult without styrene than that of PSt macroinitiator, as evidenced by stronger bimodality and higher overall polydispersity.

Synthesis of Poly(*n*-butyl acrylate)-*b*-poly(methyl methacrylate-*co*-styrene) Using ICAR ATRP. A PBA−Br macroinitiator was extended with pure MMA and with a mixture of MMA/St (10 mol %) using ICAR ATRP. ICAR is a similar process to ARGET ATRP in that it can form well-defined polymers using ppm level of Cu. The difference between the two systems is that ARGET uses a reducing agent, while ICAR uses organic radical initiators, such as AIBN, to regenerate Cu^I species. Both of these systems have been described in detail in previous reports,[29] and both can be applied for synthesis of block copolymers, although in ICAR, as in RAFT, some homopolymer should be always formed due to the generation of new chains by AIBN. In the case of performed experiments, the amount of homopolymer was negligible. The results obtained from the ICAR experiments are similar to those from the ARGET experiments. As seen in the GPC traces, there was poor initiation efficiency without styrene, Figure 6a, while with 10 mol % styrene, the PBA macroinitiator could be extended in a controlled manner, Figure 6b. These results should also be similar starting from PSt as macroinitiator.

Predici Simulations. In order to gain deeper insight into the copolymerization process, Predici software was used to kinetically model the chain extension from the PBA macroinitiator with pure MMA and with a mixture of MMA/St (10 mol %) using ICAR ATRP conditions. ICAR was used in the simulation, because the redox process in ARGET ATRP is more complex and some rate constants for the redox process are not yet available.

The GPC data of the synthesized macroinitiator PBA (M_n = 18 000, M_w/M_n = 1.12) was directly incorporated into the simulation model. The kinetic parameters used for the simulation are available in literature, and are listed in Table 2. The simulation results shown in Figure 7 closely resemble those observed in Figures 4 and 6. Much better control was observed when 10 mol % St was added into the reaction.

To obtain additional information about each polymerization process, kinetics generated from the Predici data were examined in detail. The rate constants used in the simulations are shown in Table 2. Figures 8 and 9 show concentrations and rates (determined as the product of the rate constant times the concentration of reactants) on a logarithmic scale vs conversion

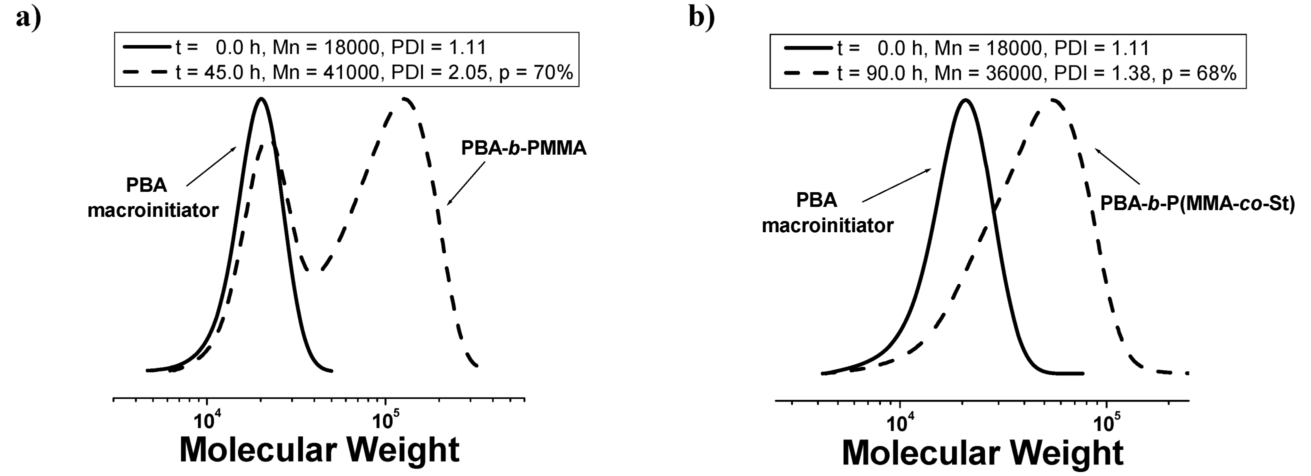

Figure 6. GPC traces of PBA−Br macroinitiator before and after chain extension with (a) MMA and (b) MMA/St copolymer using ICAR ATRP conditions: MMA/St/PBA−Br/$CuCl_2$/TPMA/AIBN = 180/20/1/0.01/0.01/0.1; $[MMA]_0 = 3.6$ M; $T = 60$ °C, in anisole (0.2 volume equivalents vs monomer).

Table 2. Parameters and Reaction Conditions Employed in Predici Simulations of ICAR ATRP MMA/St Copolymer Chain Extended from PBA−Br Macroinitiator[a]

	step	rate constant	value (M^{-1} s^{-1})
decomposition	$I_2 \rightarrow I + I$	k_{dc}[44]	1×10^{-5} (s^{-1})
initiation	$X{-}Cu^{II} + I \rightarrow Cu^{I} + IX$	k_{d2}[42]	1×10^{6}
	$PX + Cu^{I} \leftrightarrow P + X{-}Cu^{II}$	k_{act0}[45]	30
		k_{deact0}[16,45]	6×10^{7}
	$P + M1 \rightarrow P1(1)$	k_{i1}[43,46]	1.2×10^{5}
	$P + M2 \rightarrow P2(1)$	k_{i2}[43,46]	1.8×10^{5}
	$I + M1 \rightarrow IP1(1)$	k_{ii1}[43,46]	9.5×10^{5}
	$I + M2 \rightarrow IP2(1)$	k_{ii2}[43,46]	2.2×10^{5}
propagation	$P1(s) + M1 \rightarrow P1(s+1)$ $IP1(s) + M1 \rightarrow IP1(s+1)$	k_{p1}[47]	820
	$P2(s) + M1 \rightarrow P1(s+1)$ $IP2(s) + M1 \rightarrow IP1(s+1)$	k_{p2}/r_{21}[43,47]	430/0.52
	$P2(s) + M2 \rightarrow P2(s+1)$ $IP2(s) + M2 \rightarrow IP2(s+1)$	k_{p2}[47]	430
	$P1(s) + M2 \rightarrow P2(s+1)$ $IP1(s) + M2 \rightarrow IP2(s+1)$	k_{p1}/r_{12}[43,47]	820/0.46
activation	$P1X(s) + Cu^{I} \rightarrow P1(s) + X{-}Cu^{II}$ $IP1X(s) + Cu^{I} \rightarrow IP1(s) + X{-}Cu^{II}$	k_{act1}[45]	400
	$P2X(s) + Cu^{I} \rightarrow P2(s) + X{-}Cu^{II}$ $IP2X(s) + Cu^{I} \rightarrow IP2(s) + X{-}Cu^{II}$	k_{act2}[45]	20
deactivation	$P1(s) + X{-}Cu^{II} \rightarrow PX1(s) + Cu^{I}$ $IP1(s) + X{-}Cu^{II} \rightarrow IPX1(s) + Cu^{I}$	k_{deact1}[16,45]	4×10^{5}
	$P2(s) + X{-}Cu^{II} \rightarrow PX2(s) + Cu^{I}$ $IP2(s) + X{-}Cu^{II} \rightarrow IPX2(s) + Cu^{I}$	k_{deact2}[16,45]	4×10^{6}
termination	$I + I \rightarrow I{-}I$	k_{t0}[46,48]	2.5×10^{9}
	$P^* + P^* \rightarrow$ D-ATRP (P^* = P, P1, P2, IP1, IP2)	k_{tc}[49]	1×10^{8}
	$P^*(s) + P^*(r) \rightarrow$ D-ATRP(s) + DATRP(r) (P^* = P, P1, P2, IP1, IP2)	k_{td}[49]	1×10^{7}

[a] DP = 200, 50 ppm of Cu, 60 °C; PX = PolyBA-Br, M1 = MMA, M2 = St. $[M]_0/[PBA{-}X]_0/[X{-}Cu^{II}]_0/[I_2]_0 = 200/1/0.01/0.1$, $[M1]_0 + [M2]_0 = 4.11$ M. The sources of the values of rate constants (60 °C) are as follows. k_{dc}: the decomposition rate constant for free radical initiator (AIBN) at 60 °C.[44] k_{d2}: the deactivation rate constant for free radical with X−Cu^{II} species, estimated from k_{deact} for ATRP (10^5−10^8 M^{-1} s^{-1}).[42] k_{act0}, k_{act1}, k_{act2}: the activation rate constants for PBA−Br, PMMA−Br, and PSt−Br with Cu^I/Me6TREN, respectively, measured at 35 °C and extrapolated to 60 °C.[45] k_{deact0}, k_{deact1}, k_{deact2}: the deactivation rate constants for PBA−Br, PMMA−Br, and PSt−Br with Cu^IBr/Me_6TREN, respectively, calculated from k_{act}/K_{ATRP} at 35 °C and extrapolated to 60 °C.[16,45] k_{t0}: the termination rate constant for small molecular radicals.[46,48] k_{i1}, k_{i2}, k_{ii1}, and k_{ii2}: the rate constant for addition of radicals from PBA radical to MMA (k_{i1}) and St (k_{i2}), respectively; and AIBN radical to MMA (k_{ii1}) and St (k_{ii2}), respectively. Values are calculated at 60 °C from the frequency factor and activation energy taken from the literature.[43,46] k_{p1}, k_{p2} : the propagation rate constant for MMA and St, respectively. Values of k_p are taken from the literature.[47] k_{tc}, k_{td}: the termination rate constant for polymeric radicals, the combination rate constant (k_{tc}), and disproportion rate constant (k_{td}). Values are estimated from the literature.[49]

of MMA for the chain extension of PBA−Br using MMA or MMA/St (10 mol %) via ICAR ATRP. Concentrations of the macroinitiator and other dormant species are also shown on a linear scale in Figure 10. By close examination of each plot, interesting information was obtained that proved to be useful in the understanding of these processes.

The change in concentration of the reactants in the extension of PBA−Br with MMA, Figure 8, and with MMA/St (10 mol %), Figure 9, are shown in each graph as solid red lines. The overall concentration of propagating radicals (P*(all)) remains steady, and is close to the same value in each Figure, indicating the same overall polymerization rate for both systems. The disappearance of PBA−Br occurs slowly with no St present (Figure 8), with only 50% of it gone after 45% conversion of MMA is reached. PBA−Br disappears much faster when St was used (Figure 9), with 50% gone after only 7% conversion of MMA, and almost all of it disappeared after 30% MMA conversion. This can also be clearly seen in Figure 10.

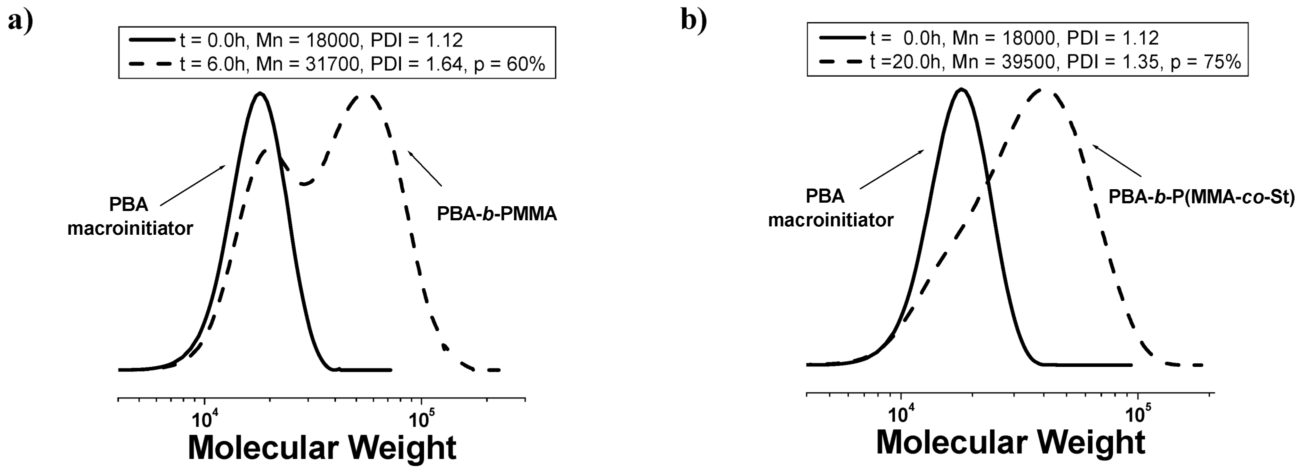

Figure 7. Predici simulation results of PBA−Br macroinitiator before and after chain extension with (a) MMA and (b) MMA/St copolymer. Experimental conditions for chain extension with MMA and 10 mol % St: MMA/St/PBA−Br/$CuCl_2$/TPMA/AIBN = 180/20/1/0.01/0.06/0.1. The kinetic parameters are listed in Table 2.

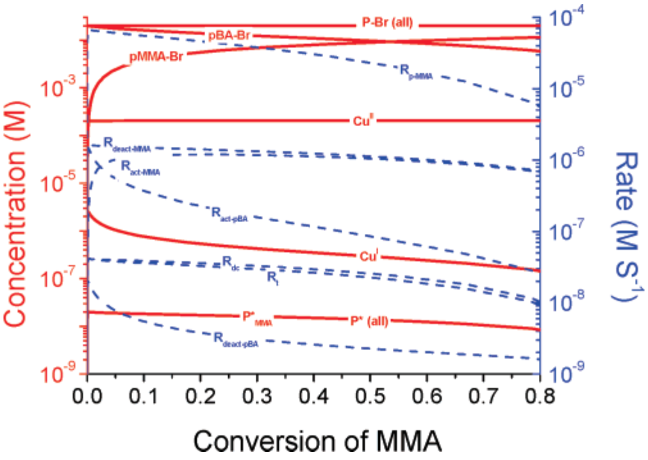

Figure 8. Predici simulation of kinetic plots for ICAR ATRP of MMA chain extended from PBA−Br macroinitiator.

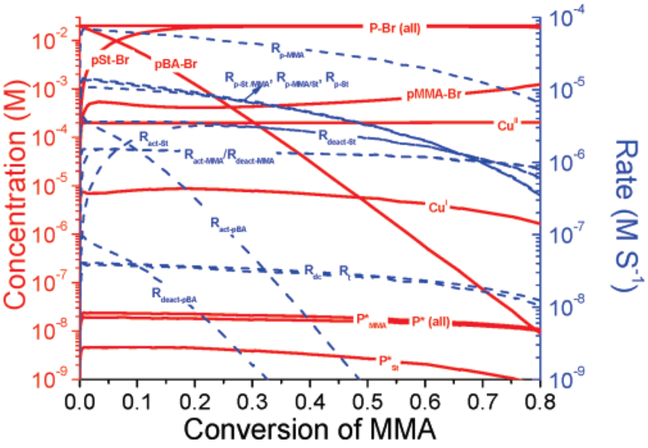

Figure 9. Predici simulation of kinetic plots for ICAR ATRP of MMA/St (10 mol %) chain extended from PBA−Br macroinitiator.

The concentration of PMMA−Br is low when St was used, because nearly all of the dormant chains are St terminated (PSt-Br). When St was not used, the concentration of PMMA−Br is higher, however it does not constitute the majority of dormant chains (P−Br (all)). This is because there is still a significant amount of PBA−Br remaining. In both systems, the concentration of Cu^{II} is essentially the same, and remains constant throughout polymerization. But, there is a significant difference in the Cu^I concentration between each system. Without St, there is about 0.5% Cu^I present. The Cu^I concentration increases about 10 times to be close to 5% with St. As will be discussed below, this increase has a prominent effect on polymerization control.

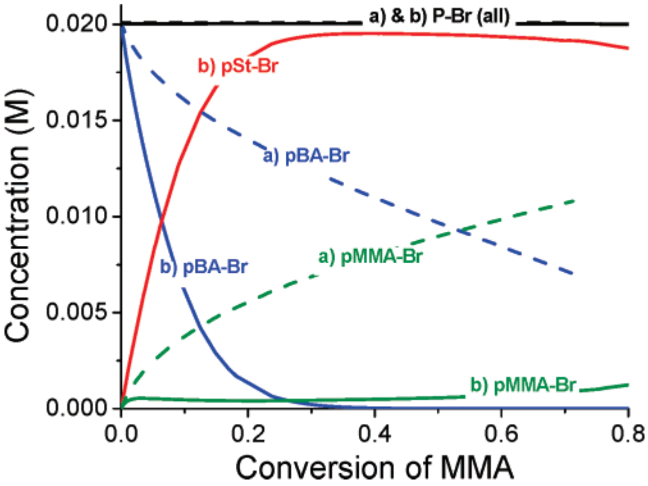

Figure 10. Predici simulation of evolution of macroinitiator and dormant species for ICAR ATRP of (a) MMA and (b) MMA/St (10 mol %) chain extended from the PBA−Br macroinitiator.

Rates of polymerization (R_p), activation of dormant chains (R_{act}), deactivation of growing chains (R_{deact}), termination (R_t), decomposition of AIBN (R_{dc}), and cross-propagation for the MMA/St system (either $R_{p-St/MMA}$ or $R_{p-MMA/St}$) are shown as the dashed blue lines in Figures 8 and 9. After the initial stages of each simulation, the rate of polymerization for MMA (R_{p-MMA}) is on average no more than 30 times the rates for activation ($R_{act-MMA}$) and deactivation ($R_{deact-MMA}$) for an MMA-terminated chain. This means about 30 monomer units are added at each activation step, corresponding to a well controlled system. The $R_{act-MMA}$ and $R_{deact-MMA}$ do not reach equilibrium until about 20% conversion of MMA is reached, when St was not used. These two values reach equilibrium much sooner with St present, occurring at less than 2% MMA conversion. The activation (R_{act-St}) and deactivation ($R_{deact-St}$) for St, however, are not at equilibrium until 20% conversion of MMA. Rates of activation ($R_{act-PBA}$) and deactivation ($R_{deact-PBA}$) of the PBA macroinitiator are not equilibrated in either case, but the difference between the two is far less when St is used as comonomer. Rates of crosspropagation from PMMA to PSt ($R_{p-MMA/St}$) and from PSt to PMMA ($R_{p-St/MMA}$) reach equilibrium at 20% conversion of MMA, and are essentially the same throughout the reaction. Last, R_{dc} is essentially the same as R_t in both simulations, as in a typical ICAR homopolymerization.[29]

To summarize these observations, the rate of generation of new radicals (decomposition of AIBN) is similar to the rate of termination. This means there is a steady concentration of radicals, confirmed also by the constant value of [P*] observed on the graphs. These values are the same in both Figures 8 and 9, so there is the same polymerization rate for each system. The presence of St does not slow down the polymerization. Another important observation was the increased levels of Cu^I in the simulation with St. In ICAR homopolymerization, the ratio $[Cu^{II}]/[Cu^I]$ is determined by the ATRP equilibrium defined by the catalytic system. In ICAR copolymerization with the same catalyst, $[Cu^{II}]/[Cu^I]$ ratio is determined by the ATRP equilibrium constants of comonomers provided that the system is under full equilibration. In the simulation with St, crosspropagation is fast and is rapidly equilibrated. The rates of activation and deactivation are also equilibrated, although they are initially higher for PSt than for PMMA. This predominantly affects Cu^I concentration. Since there is the same concentration of radicals and dormant chains in each system, the smaller K_{ATRP} for PSt provides a larger Cu^I concentration in the simulation with St. As there is 10 times more Cu^I in this case, the rate of activation of PBA macroinitiator increases 10 times. Therefore, there is a 10-fold improvement in initiation efficiency when St is used as a comonomer. Thus, it seems that the main reason for enhanced crosspropagation efficiency is higher concentration of Cu^I, caused by the presence of St dormant species that has a lower K_{ATRP}.

Conclusions

The successful synthesis of block copolymers via ARGET or ICAR ATRP where polyacrylate or polystyrene macroinitiators are used as the first block, with a methacrylate-rich second block has been reported. As halogen exchange could not be used for the ARGET system, styrene was used as a comonomer in the extension polymerization to provide efficient initiation. Model studies with small molecule acrylate and styrene-based initiators as were used to determine that only 10 mol % of styrene was needed to provide sufficient control. As evidenced by GPC, the extensions from poly(*n*-butyl acrylate) and polystyrene macroinitiators were successful. Predici simulations also confirmed that the presence of styrene significantly improved initiation efficiency, predominantly due to higher concentration of Cu^I and consequently faster activation of BA dormant species. This method extends the application of ARGET and ICAR ATRP for block copolymer synthesis.

Acknowledgment. The authors acknowledge NSF DMR 05-49353 and NSF Graduate Research Fellowship (for L.M.).

References and Notes

(1) Hadjichristidis, N.; Pispas, S.; Floudas, G. *Block copolymers: synthetic strategies, physical properties, and applications*; John Wiley & Sons, Inc.: Hoboken, NJ, 2003.

(2) Hamley, I. W. *The Physics of block copolymers*; Oxford University Press: Oxford, U.K., 1998.

(3) Various living polymerizations and their application to the synthesis of block copolymers are covered in the following review articles: (a) Matyjaszewski, K. M.; A. H. E. *Prog. Polym. Sci.* **2006**, *31*, 1039−1040. (b) Smid, J.; Van Beylen, M.; Hogen-Esch, T. E. *Prog. Polym. Sci.* **2006**, *31*, 1041−1067. (c) Hadjichristidis, N.; Iatrou, H.; Pitsikalis, M.; Mays, *J. Prog. Polym. Sci.* **2006**, *31*, 1068−1132. (d) Yagci, Y.; Tasdelen, M. A. *Prog. Polym. Sci.* **2006**, *31*, 1133−1170. (e) Bielawski, C. W.; Grubbs, R. H. *Prog. Polym. Sci.* **2007**, *32*, 1−29. (f) Domski, G. J.; Rose, J. M.; Coates, G. W.; Bolig, A. D.; Brookhart, M. *Prog. Polym. Sci.* **2007**, *32*, 30−92. (g) Braunecker, W. A.; Matyjaszewski, K. *Prog. Polym. Sci.* **2007**, *32*, 93−146. (h) Yokozawa, T.; Yokoyama, A. *Prog. Polym. Sci.* **2007**, *32*, 147−172. (i) Baskaran, D.; Mueller, A. H. E. *Progr. Polym. Sci.* **2007**, *32*, 173−219. (j) Goethals, E. J.; Du Prez, F. *Prog. Polym. Sci.* **2007**, *32*, 220−246. (k) Penczek, S.; Cypryk, M.; Duda, A.; Kubisa, P.; Slomkowski, S. *Progr. Polym. Sci.* **2007**, *32*, 247−282.

(4) Hawker, C. J.; Bosman, A. W.; Harth, E. *Chem. Rev.* **2001**, *101*, 3661−3688.

(5) Chiefari, J.; Chong, Y. K.; Ercole, F.; Krstina, J.; Jeffery, J.; Le, T. P. T.; Mayadunne, R. T. A.; Meijs, G. F.; Moad, C. L.; Moad, G.; Rizzardo, E.; Thang, S. H. *Macromolecules* **1998**, *31*, 5559−5562.

(6) Wang, J.-S.; Matyjaszewski, K. *J. Am. Chem. Soc.* **1995**, *117*, 5614−5615.

(7) Kato, M.; Kamigaito, M.; Sawamoto, M.; Higashimura, T. *Macromolecules* **1995**, *28*, 1721−1723.

(8) Kamigaito, M.; Ando, T.; Sawamoto, M. *Chem. Rev.* **2001**, *101*, 3689−3745.

(9) Matyjaszewski, K.; Xia, J. *Chem. Rev.* **2001**, *101*, 2921−2990.

(10) Braunecker, W. A.; Matyjaszewski, K. *Prog. Polym. Sci.* **2007**, *32*, 93−146.

(11) Braunecker, W. A.; Matyjaszewski, K. *J. Mol. Catal. A, Chem.* **2006**, *254*, 155−164.

(12) Coessens, V.; Pintauer, T.; Matyjaszewski, K. *Prog. Polym. Sci.* **2001**, *26*, 337−377.

(13) Davis, K. A.; Matyjaszewski, K. *Adv. Polym. Sci.* **2002**, *159*, 1−166.

(14) Wang, J.-S.; Matyjaszewski, K. *Macromolecules* **1995**, *28*, 7572−7573.

(15) Wang, J.-L.; Grimaud, T.; Shipp, D. A.; Matyjaszewski, K. *Macromolecules* **1998**, *31*, 1527−1534.

(16) Tang, W.; Tsarevsky, N. V.; Matyjaszewski, K. *J. Am. Chem. Soc.* **2006**, *128*, 1598−1604.

(17) Matyjaszewski, K.; Shipp, D. A.; McMurtry, G. P.; Gaynor, S. G.; Pakula, T. *J. Polym. Sci., Part A: Polym. Chem.* **2000**, *38*, 2023−2031.

(18) Shipp, D. A.; Wang, J.-L.; Matyjaszewski, K. *Macromolecules* **1998**, *31*, 8005−8008.

(19) Hong, S. C.; Pakula, T.; Matyjaszewski, K. *Macromol. Chem. Phys.* **2001**, *202*, 3392−3402.

(20) Hong, S. C.; Pakula, T.; Matyjaszewski, K. *Polym. Mater. Sci. Eng.* **2001**, *84*, 767−768.

(21) Tsarevsky, N. V.; Sarbu, T.; Goebelt, B.; Matyjaszewski, K. *Macromolecules* **2002**, *35*, 6142−6148.

(22) Ramakrishnan, A.; Dhamodharan, R. *Macromolecules* **2003**, *36*, 1039−1046.

(23) Tang, C.; Kowalewski, T.; Matyjaszewski, K. *Macromolecules* **2003**, *36*, 1465−1473.

(24) Tsarevsky, N. V.; Cooper, B. M.; Wojtyna, O. J.; Jahed, N. M.; Gao, H.; Matyjaszewski, K. *Polym. Prep.* (*Am. Chem. Soc., Div. Polym. Chem.*) **2005**, *46*, 249−250.

(25) Huang, J.; Jia, S.; Siegwart, D. J.; Kowalewski, T.; Matyjaszewski, K. *Macromol. Chem. Phys.* **2006**, *207*, 801−811.

(26) Dong, H.; Tang, W.; Matyjaszewski, K. *Macromolecules* **2007**, *40*, 2974−2977.

(27) Jakubowski, W.; Matyjaszewski, K. *Angew. Chem., Int. Ed.* **2006**, *45*, 4482−4486.

(28) Jakubowski, W.; Min, K.; Matyjaszewski, K. *Macromolecules* **2006**, *39*, 39−45.

(29) Matyjaszewski, K.; Jakubowski, W.; Min, K.; Tang, W.; Huang, J.; Braunecker, W. A.; Tsarevsky, N. V. *Proc. Natl. Acad. Sci. U.S.A.* **2006**, *103*, 15309−15314.

(30) (a) Pietrasik, J.; Dong, H.; Matyjaszewski, K. *Macromolecules* **2006**, *39*, 6384−6390. (b) Min, K.; Gao, H.; Matyjaszewski, K. *Macromolecules* **2007**, *40*, 1789−1791.

(31) Tang, H.; Arulsamy, N.; Radosz, M.; Shen, Y.; Tsarevsky, N. V.; Braunecker, W. A.; Tang, W.; Matyjaszewski, K. *J. Am. Chem. Soc.* **2006**, *128*, 16277−16285.

(32) Tang, H.; Radosz, M.; Shen, Y. *Macromol. Rapid Commun.* **2006**, *27*, 1127−1131.

(33) Matyjaszewski, K.; Davis, K.; Patten, T. E.; Wei, M. *Tetrahedron* **1997**, *53*, 15321−15329.

(34) Lutz, J.-F.; Matyjaszewski, K. *Macromol. Chem. Phys.* **2002**, *203*, 1385−1395.

(35) Lutz, J.-F.; Matyjaszewski, K. *J. Polym. Sci., Part A: Polym. Chem.* **2005**, *43*, 897−910.

(36) Charleux, B.; Nicolas, J.; Guerret, O. *Macromolecules* **2005**, *38*, 5485−5492.

(37) Nicolas, J.; Dire, C.; Mueller, L.; Belleney, J.; Charleux, B.; Marque, S. R. A.; Bertin, D.; Magnet, S.; Couvreur, L. *Macromolecules* **2006**, *39*, 8274−8282.

(38) (a) Tyeklar, Z.; Jacobson, R. R.; Wei, N.; Murthy, N. N.; Zubieta, J.; Karlin, K. D. *J. Am. Chem. Soc.* **1993**, *115*, 2677. (b) Xia, J.; Matyjaszewski, K. *Macromolecules* **1999**, *32*, 2434−2437.

(39) Barner-Kowollik, C.; Buback, M.; Egorov, M.; Fukuda, T.; Goto, A.; Olaj, O. F.; Russell, G. T.; Vana, P.; Yamada, B.; Zetterlund, P. B. *Prog. Polym. Sci.* **2005**, *30*, 605−643.

(40) Beuermann, S.; Buback, M. *Prog. Polym. Sci.* **2002**, *27*, 191−254.

(41) Madruga, E. L. *Prog. Polym. Sci.* **2002**, *27*, 1879−1924.

(42) Matyjaszewski, K.; Paik, H.-j.; Zhou, P.; Diamanti, S. J. *Macromolecules* **2001**, *34*, 5125−5131.

(43) Brandrup, J.; Immergut, E. H.; Grulke, E. A. *Polymer Handbook*, 4th ed.; John Wiley and Sons, Inc.: New York, 1999.

(44) Bamford, C. H.; Tipper, C. F. H. *Comprehensive Chemical Kinetics, Vol. 14A: Free Radical Polymerization*; Elsevier: Amsterdam, The Netherlands, 1976.

(45) Tang, W.; Matyjaszewski, K. *Macromolecules* **2007**, *40*, 1858−1863.

(46) Fischer, H.; Radom, L. *Angew. Chem., Int. Ed.* **2001**, *40*, 1340−1371.

(47) Buback, M.; Gilbert, R. G.; Hutchinson, R. A.; Klumperman, B.; Kuchta, F.-D.; Manders, B. G.; O'Driscoll, K. F.; Russell, G. T.; Schweer, J. *Macromol. Chem. Phys.* **1995**, *196*, 3267−3280.

(48) Fischer, H.; Paul, H. *Acc. Chem. Res.* **1987**, *20*, 200−206. Shipp, D. A.; Matyjaszewski, K. *Macromolecules* **1999**, *32*, 2948−2955.

(49) Buback, M.; Egorov, M.; Gilbert, R. G.; Kaminsky, V.; Olaj, O. F.; Russell, G. T.; Vana, P.; Zifferer, G. *Macromol. Chem. Phys.* **2002**, *203*, 2570−2582.

MA071130W